An assessment of sanidine from the Fire Clay tonstein as a Carboniferous ^{40}Ar/^{39}Ar monitor standard and for inter-method comparison to U-Pb zircon geochronology

Malka L. Machlus[a,b,*], Erin K. Shea[c,1], Sidney R. Hemming[a,d], Jahandar Ramezani[c], E. Troy Rasbury[e]

[a] *Lamont-Doherty Earth Observatory of Columbia University, Palisades, NY 10964, United States of America*
[b] *Department of Physical Sciences, Kingsborough Community College, City University of New York, Brooklyn, NY 11235, United States of America*
[c] *Earth, Atmospheric, and Planetary Science, Massachusetts Institute of Technology, Cambridge, MA 02139, United States of America*
[d] *Department of Earth and Environmental Sciences, Columbia University, New York, NY, United States of America*
[e] *Department of Geosciences, Stony Brook University, Stony Brook, NY, 11794, United States of America*

ARTICLE INFO

ABSTRACT

Radioisotopic geochronology applied to the high-resolution calibration of Earth history requires a set of synthetic and natural reference materials for both ^{40}Ar/^{39}Ar and U-Pb techniques that permit both inter-laboratory and inter-technique comparisons. The sanidine- and zircon-bearing Carboniferous Fire Clay tonstein provides a potential natural Paleozoic reference for these two widely used radioisotopic systems. Here we report results for both radioisotopic systems, examining the suitability of this tonstein as a geochronologic reference. Sanidine crystals from the Fire Clay and co-irradiated monitors from eight irradiation positions were divided into eleven ^{40}Ar/^{39}Ar experiments. Single-grain sanidine ^{40}Ar/^{39}Ar analyses (n = 263) of the simplest 9 experiments have internal 2σ uncertainties at the ± 1 Myr level (± 0.3%), with a range of dates between ~315 and ~317 Ma (~1% precision), similar to the observed dispersion in the Fish Canyon sanidine monitor dates. Forty-one U-Pb analyses by the CA-ID-TIMS method on carefully selected single Fire Clay tonstein zircons have produced ^{206}Pb/^{238}U dates with an average 2σ precision of ± 0.23 Myr (0.14%). Our Fire Clay preferred mean ^{40}Ar/^{39}Ar date of 315.36 ± 0.10 Ma (± 1.10 Ma: fully propagated 2σ uncertainty, relative to a Fish Canyon age of 28.201 Ma) is consistent with our weighted mean ^{206}Pb/^{238}U zircon date of 314.629 ± 0.039 Ma (± 0.35 Ma: fully propagated 2σ uncertainty; n = 27). The good single-crystal reproducibility of the sanidine data and the overall consistency between the two chronometers suggest that the tonstein holds promise as a Paleozoic age reference material.

1. Introduction

As geochronometers become increasingly more precise we are presented with the issue of age inaccuracy stemming from bias between chronometers and laboratories. ^{40}Ar/^{39}Ar in sanidine and U-Pb in zircon are widely applied radioisotopic chronometers for the Geologic Time Scale (Ogg et al., 2016; Schmitz, 2012). Recent advances in U-Pb geochronology, such as the EARTHTIME community-driven production and distribution of calibrated U-Pb isotopic tracers for ID-TIMS analyses (Condon et al., 2015; McLean et al., 2015) have highlighted the need for reciprocal improvements in ^{40}Ar/^{39}Ar geochronology, cross-calibration between the two chronometers, and their seamless integration into the Geologic Time Scale.

In order to achieve the EARTHTIME initiative's goal of accurate and precise sequencing of geologic events at the 0.1% level, the ^{40}Ar/^{39}Ar and U-Pb communities require a set of samples that permit inter-laboratory and inter-technique comparisons. Natural zircon and sanidine reference materials play a critical role for these comparisons, but are currently limited in number. Plešovice (Sláma et al., 2008), R33, and Temora 2 (Black et al., 2004) are commonly used for zircon, whereas Fish Canyon, Alder Creek, and Taylor Creek are the most frequently used sanidine standards (Renne et al., 1998); we know of none that are available from the same volcanic eruption for both ^{40}Ar/^{39}Ar and U-Pb chronometers without evident complexity in one of the chronometers.

There is currently no recognized Paleozoic sanidine monitor standard for ^{40}Ar/^{39}Ar geochronology let alone a monitor standard older than ~30 Ma, and there is a significant need for samples that contain both sanidines and zircons for inter-laboratory and -method refinements. The sanidine- and zircon-bearing Carboniferous Fire Clay tonstein, a voluminous ash bed from the Appalachian Basin, provides potential natural Paleozoic monitor for ^{40}Ar/^{39}Ar geochronology and a reference material for inter-method comparison between ^{40}Ar/^{39}Ar and U-Pb. Here we report the results of 263 single-grain sanidine ^{40}Ar/^{39}Ar analyses from eight irradiation positions and 41 single-zircon U-Pb CA-ID-TIMS analyses from samples of the Fire Clay tonstein, introducing the Fire Clay sanidine as a natural reference material for ^{40}Ar-^{39}Ar geochronology with the advantage of cross-calibration with the U-Pb system.

1.1. ^{40}Ar/^{39}Ar and U-Pb geochronology

^{40}Ar/^{39}Ar geochronology relies on the assumption of a known standard with a precisely and accurately determined absolute age to which unknowns are referenced. Sanidine from the Oligocene Fish Canyon tuff is the most commonly applied standard, despite reported ages that range from 28.393 (Ganerød et al., 2011) to 27.79 (Cebula et al., 1986) and evidence for complexity in the eruptive system for the Fish Canyon tuff (e.g., Lipman and Bachmann, 2015, and references therein). In the ^{40}Ar/^{39}Ar system, radioactive ^{40}K undergoes a branched decay to ^{40}Ar and ^{40}Ca, and significant uncertainties are associated with their decay constants (Min et al., 2000; Renne et al., 2011, 2010). U-Pb geochronology by in situ (microbeam) techniques also requires chemically and isotopically well-characterized reference materials including natural mineral standards. In contrast, U-Pb dates by the isotope dilution method of U-bearing minerals such as zircon are calibrated against 'tracer' solutions (usually ^{205}Pb $\pm$ ^{202}Pb and ^{235}U $\pm$ ^{233}U) of precisely calibrated isotopic abundances. These tracer solutions allow for U and Pb isotopic ratios in the samples to be accurately determined, and these ratios can be traced back to SI units through weights and measures (Condon et al., 2015; McLean et al., 2015). Additional advantages of the U-Pb system include the precisely and accurately determined ^{238}U half-life (Jaffey et al., 1971) and recent improvements in the ratio of the ^{235}U and ^{238}U decay constants (Mattinson, 2010). Recent efforts made by the EARTHTIME U-Pb community have involved development of standard 'age solutions' of known composition, made available to the community, re-evaluation of the isotopic composition of natural uranium (Hiess et al., 2012) and the re-determination of the isotopic composition of some commonly used uranium reference materials which underpin the calibration experiments and results (Condon et al., 2010). With increased precision and accuracy of U-Pb zircon dates, subtle complexities in the U-Pb systematics of magmatic systems become significant and need to be addressed. Improvements in the precision and accuracy of ^{40}Ar/^{39}Ar dating will lead to improved ability to scrutinize potential geological complexity in both systems.

1.2. Fire Clay tonstein

The Pennsylvanian Fire Clay tonstein is a kaolinized volcanic air-fall ash bed that covers a minimum of 37,000 km^2 in eastern Kentucky, West Virginia, and parts of Tennessee and Virginia (Fig. 1; Lyons et al., 1992). The geographic range of this eruptive ash has made it a critical lithostratigraphic marker in the Appalachian Basin. The tonstein is commonly found as a 4 to 20 cm thick layer near the base of the Fire Clay coal bed, although thicknesses up to 39 cm have been reported (Huddle and Englund, 1966; Stevens, 1979; Chesnut, 1985).

Because of its significance as a stratigraphic marker bed, the Fire Clay tonstein has been particularly well-mapped and studied (e.g., Huddle and Englund, 1966; Kunk and Rice, 1994; Lyons et al., 2006, 1992; Rice et al., 1994; Stevens, 1979; Wanless, 1946). It is comprised of well-crystallized kaolinite with 3–5% accessory minerals (Rice et al.,

1994). The tonstein is described as dark brownish-grey in color, beds exhibit conchoidal fracture and show a waxy luster (Kunk and Rice, 1994). Thin-section and single-mineral studies indicate a volcanic origin for the tonstein and previous workers have found no evidence for authigenic or detrital phenocrysts (Kunk and Rice, 1994). ^{40}Ar/^{39}Ar geochronology on large, multi-crystal, step-heated samples of sanidine from across the available exposures of the tonstein has shown remarkable reproducibility (Kunk and Rice, 1994), supporting the hypothesized volcanic origin for these phenocrysts. The eruptive source of the Fire Clay ash has been suggested to be the North Carolina piedmont (Rice et al., 1994; Sinha and Zietz, 1982) or the present-day Gulf of Mexico (Lyons et al., 1992).

Previous ^{40}Ar/^{39}Ar geochronology on multi-grain sanidine separates from the Fire Clay tonstein gave ages from 312.1 $\pm$ 1 Ma (Lyons et al., 1992: four separate step heating experiments, including two of Hess et al., 1988); to 310.9 $\pm$ 0.8 Ma (seven step heated sanidine samples of ~100 mg each in Kunk and Rice, 1994). The data from Kunk and Rice (1994) has a range of reported plateaus of 310.25 $\pm$ 0.55 Ma to 311.38 $\pm$ 0.55 Ma for samples collected over a 300 km distance, showing remarkable internal consistency. Note that if Kunk and Rice (1994) ages are converted from Fish Canyon monitor age of 27.79 Ma to an improved age of 28.201 Ma and from ^{40}K decay constants of Steiger and Jäger (1977) to those of Min et al. (2000), this age range translates to 314.83 Ma to 315.98 Ma (converted by ArAr software of Mercer and Hodges, 2016).

Early U-Pb geochronology from the Fire Clay tonstein involved analysis of multi-grain (103–145 mg) fractions of untreated zircon by the ID-TIMS method, each based on a different tonstein sample from West Virginia, Virginia, Tennessee and Kentucky. These analyses produced highly discordant U-Pb results due to the widespread presence of xenocrystic components; the four samples defined a roughly linear array with concordia intercepts at 344 $\pm$ 35 Ma and 1224 $\pm$ 150 Ma (MSWD = 15). The results did not allow any meaningful comparison between U-Pb and the ^{40}Ar/^{39}Ar chronometers at the time (Rice et al., 1994). Lyons et al. (2006) reported five single-zircon U-Pb analyses by the ID-TIMS method on air-abraded zircons from a sample of the Fire Clay tonstein from Pike Co., Kentucky. Four of these analyses were highly discordant due to zircon inheritance. The single, youngest ^{206}Pb/^{238}U date of 314.6 $\pm$ 0.9 Ma (2σ) was interpreted as the age of deposition of the Fire Clay ash (Lyons et al., 2006). The proximity of the latter U-Pb date to the published ^{40}Ar/^{39}Ar geochronology suggested that the Fire Clay tonstein held promise as a potential Paleozoic reference material for both systems.

2. Materials and methods

2.1. Mineral separation

Three samples (RH1, RV5 and RS1) were collected from the Fire Clay tonstein within close proximity to the locations of samples RH and RV (Kentucky) and RS (West Virginia) of Kunk and Rice (1994), respectively (Fig. 1). Kaolinite matrix of the Fire Clay tonstein is difficult to separate from the enclosed phenocrysts using standard methods of disaggregation (e.g., Kunk and Rice, 1994) and therefore after the initial crushing to particles smaller than 2 mm the samples were subjected to different experiments of mineral extraction and cleaning (see Appendix A and experiments listed in Table A.1). We found the best technique to be one that uses DMSO (dimethyl sulfoxide) solution for disaggregating phenocrysts (Kunk and Rice, 1994; Triplehorn, 2002; Triplehorn et al., 2002). This method guarantees almost 100% recovery of relatively clean phenocrysts. Additional cleaning methods were applied to a subset of sanidine crystals with persistent thin coatings or spots of kaolinite (e.g., Fig. 2B). These additional methods include: leaching with weak hydrofluoric (HF) acid (see Appendix A and Table A.1) and 2-step heating during analysis (described in Section 2.2 below).
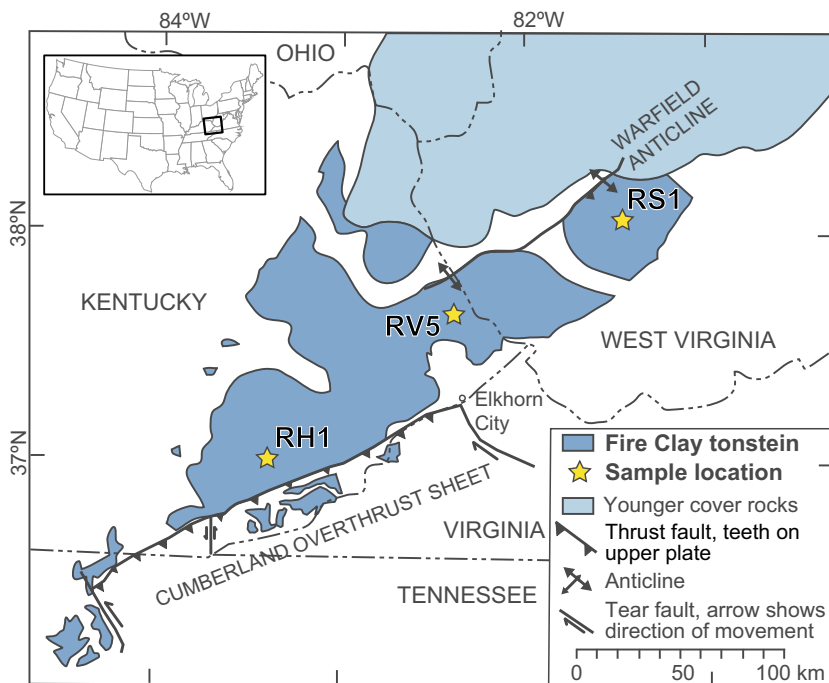
Fig. 1. Simplified geologic map showing the geographic extent of exposures of the Fire Clay tonstein in the southern Appalachians of eastern North America. A rectangle on an inset map of the contiguous United States marks the location of this geologic map. Modified from Fig. 2 of Rice et al. (1994).
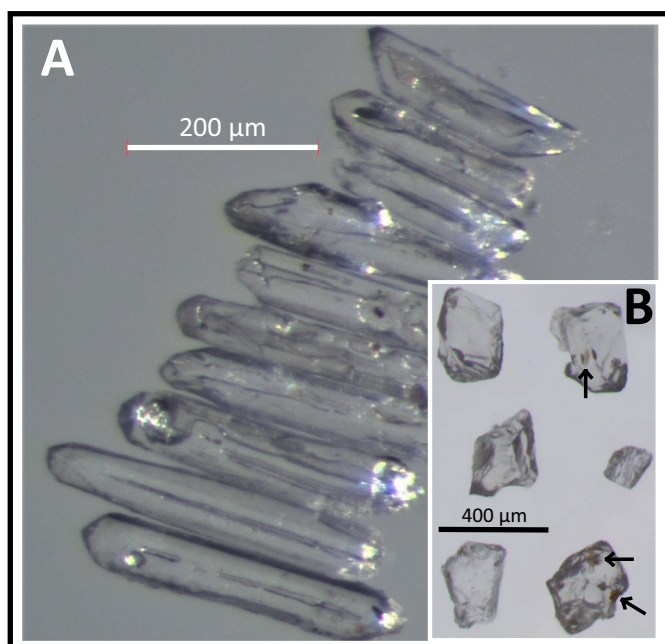

Fig. 2. Binocular microscope images of prismatic zircon (A) and sanidine (B) grains separated for analysis from the Fire Clay tonstein samples RH1 and RV5, respectively. Note the axial glass inclusions in zircons, as well as dark spots of kaolinite on sanidines (arrows). Sanidines in B are relatively clean crystals compared to some grains coated with a thin kaolinite film and with larger attached kaolinite aggregates.

After disaggregation, sanidines were concentrated with heavy liquids, sieved to size fraction > 250 μm, and hand-picked under a binocular microscope. Most sanidines are subhedral (e.g., Fig. 2B) and between 250 and 355 μm in size, although larger crystals of 355–850 μm are present. A minority population of sanidine crystals has a platy morphology.

Zircon crystals were concentrated with high-density liquids and hand-picked under a binocular microscope based on their crystal habit and morphology. Zircons from the Fire Clay tonstein range from equant to highly elongate prismatic crystals with length-to-width ratios as high as 10:1 (Fig. 2A). Many equant crystals are metamict and/or show evidence for xenocrystic cores (Rice et al., 1994). Effort was made to select prismatic zircons with elongate glass (melt) inclusions parallel to their long ('c') axis for analysis (Fig. 2A) as these have proven less likely to contain inherited cores (Ramezani et al., 2011). A few additional equant zircons were also analyzed in order to explore the xenocrystic component.

2.2. $^{40}Ar/^{39}Ar$

Sanidines were irradiated in three separate batches (irradiations numbered 29, 32, 34), each with a 10-hour duration in the Cd lined facility (CLICIT) at the Oregon State University Reactor. Each irradiation included several stacked irradiation disks, identified by appended letter (for example 29B; Fig. A.1). Fish Canyon sanidines were co-irradiated with other crystals in each pit (Tables 1 and A.1). Additional monitor standards were added to some irradiation pits, including Taylor Creek sanidine and GA1550 biotite (Renne et al., 1998), as well as two internal lab standards (sanidines): Peach Springs tuff (cima) provided by Brent Turrin, and Miocene Ignimbrite TS-1a provided by Matt Heizler (Fig. A.1). Monitor standards were provided by Matt Heizler as part of the EARTHTIME Argon inter-lab comparison experiment (Heizler and the EARTHTIME working group, 2005).

Irradiated samples were analyzed using the fully automated Lamont-Doherty Earth Observatory (LDEO) AGES VG-5400 noble gas mass spectrometer. Individual crystals were fused using a CO_2 laser at varying power levels and gases released from the heating of samples were scrubbed of reactive gases by exposure to Zr-Al sintered metal alloy getters. Isotopic ratios were determined using the MassSpec program, developed by A. Deino (Berkeley Geochronology Laboratory). Measurements were made by peak hopping on a Balzers multiplier in analogue mode. At these conditions, the ^{40}Ar signal was approximately 1×10^{-9} amps for 4×10^{-14} mol of atmospheric Ar.

Crystals were fused at the following laser power levels within three

experiment types: total fusion, 2-step cleaning and step heating spectrum. Most crystals underwent total fusion at a power of 7 W. Smaller group of crystal underwent cleaning by 2-step heating with low-power steps at 0.1 W for all single crystals (A steps), followed by 7 W fusions for the same crystals (B steps). When successful, this cleaning yields A-steps with low radiogenic Ar (low ^{39}Ar, low ^{40}Ar*) and typically widely spread dates, whereas B-steps are highly radiogenic (high ^{40}Ar*), have narrow distribution of dates with much higher ^{39}Ar compared to the A-steps. Typically, only B-steps are used for weighted mean age calculation. These two fusion styles are distinguished by the same symbols/color in all plots. Total fusion analyses plot as black circles/black curve, B-steps are plotted as red squares/red curve (lower curves compared to total fusions and grey in greyscale print), whereas A-step are marked as green triangles/green curve (Appendix A only). Multi-crystal sanidine aliquots of the Fire Clay tonstein were also analyzed at varying power levels of 0.1–7 W within step heating spectra experiments.

^{40}Ar/^{39}Ar data were corrected for backgrounds, mass discrimination and nuclear interferences. Background and mass discrimination corrections were based on time series of blanks and air pipettes (respectively) run throughout the interval of the analyses (isotopic abundance of atmospheric Ar are from Lee et al., 2006). The nuclear interference corrections were based on production ratios for the Oregon State reactor (Renne et al., 1998). Individual dates (e.g., Table A.2) are reported with ± 1σ analytical uncertainties relative to Fish Canyon monitor age of 28.201 (Kuiper et al., 2008) and using the decay constants of Min et al. (2000). J-values were calculated from Fish Canyon sanidine monitor co-irradiated in the same irradiation pit as the unknowns and other monitor standards.

Reported uncertainties are of three types: (1) analytical without J-values that can only be compared to co-irradiated monitor standard analyses from the same irradiation pit. These uncertainties allow direct comparison of the spread of individual dates for tonstein and monitor grains, and are calculated without the uncertainty associated with the weighted mean J-value for the corresponding irradiation pit and without irradiation parameters uncertainties; (2) analytical uncertainties that incorporate the J-value uncertainty, and allow comparison to any ^{40}Ar/^{39}Ar date reported relative to Fish Canyon monitor age of 28.201 Ma calculated with decay constants of Min et al. (2000). These uncertainties are required when comparing analyses from different irradiation pits, such as some of the experiments reported here; and (3) full external (total) uncertainties that include decay constants and monitor standard calibration uncertainties and allow comparison to U-Pb dates. The latter two uncertainty types and reported mean ages were calculated from R values by equations of Karner and Renne (1998), Renne et al. (1998) and modified equations of Kuiper et al. (2008) to include $R^{FiC}/_{FC}$ values reported here (FiC: Fire Clay; FC: Fish Canyon; Table 1).

Both J-values and weighted-mean-date calculations excluded some analyses. Statistical exclusion of analyses was based on two filters available in the MassSpec program: (1) "best contiguous group" (BCG) selects the largest contiguous group that has a mean square weighted deviation (MSWD) value within the 95% confidence interval for the respective group size and (2) "nMAD" deletes analyses that have median absolute deviations about the median beyond the cutoff n. When MSWD probability was < 0.05, BCG filter was applied. Both 1.5MAD/2MAD filters were noted. In all cases when BCG filter applied, either the same eliminations were selected by 2MAD filter, or the calculated ages obtained with BCG and 2MAD filters had different eliminations but overlapped within 2σ. Both MSWD probabilities, before and after elimination, are listed in Table A.2, as well as exclusion criteria specific to individual analyses such as high Ca/K ratio and low % radiogenic ^{40}Ar.

2.3. U-Pb

Zircons selected for U-Pb analysis were pre-treated by a chemical

Table 1
Summary of the Fire Clay tonstein and Fish Canyon monitor sanidine experiments.

Experiment		Fish Canyon tuff monitor							Fire Clay tonstein								$R^{FiC}/_{FC}$[a]			
Irradiation/Sample[b]	Run ID	J	± 1σ[c]	Age (Ma)	± 1σ[c] wo J	MSWD	n/tot[d]		Age (Ma)	± 1σ[c] wo J	± 1σ[c] w J	± 1σ total	MSWD	n/tot[d]			$R^{FiC}/_{FC}$	± 1σ	± %
29B9/RH1	12137	**2.5806E−03**	**5.8E−07**	**28.201**	**0.006**	1.24	**14/14**		315.27	**0.09**	**0.11**	0.56	1.40	30/32			12.1062	4.7E−03	0.04%
29A6/RH1	12170	2.5809E−03	8.6E−07	28.201	0.009	0.98	17/17		315.90	0.13	0.16	0.57	1.49	15/15			12.1324	6.7E−03	0.06%
32C6/RH1	12200[e]	2.6161E−03	9.8E−07	28.201	0.010	1.57	12/16		316.30	0.05	0.12	0.56	1.26	68/76			12.1495	5.1E−03	0.04%
32C10/RH1	12201	**2.6040E−03**	**8.6E−07**	**28.200**	**0.009**	1.49	**12/15**		315.42	**0.06**	**0.11**	0.56	1.27	53/53			12.1124	4.7E−03	0.04%
34C4/RH1	12401	2.5891E−03	8.1E−07	28.200	0.009	1.60	16/19		316.06	0.10	0.14	0.56	1.34	20/20			12.1392	5.8E−03	0.05%
34C6/RV5	12402	2.5933E−03	9.3E−07	28.201	0.010	1.68	12/14		315.56	0.12	0.16	0.57	1.60	18/19			12.1186	6.6E−03	0.05%
34C12/RS1	12403	2.5868E−03	8.1E−07	28.201	0.009	1.38	15/17		315.49	0.08	0.12	0.56	1.17	36/36			12.1155	5.1E−03	0.04%
34C1/RH1	12490	2.5931E−03	8.1E−07	28.201	0.009	1.09	19/20		315.28	0.16	0.18	0.57	1.58	12/12			12.1067	7.7E−03	0.06%

Our preferred age for the Fire Clay tonstein is calculated from $R^{FiC}/_{FC}$ = arithmetic mean of **bold** individual $R^{FiC}/_{FC}$ values ± 1 standard error of the mean = 12.1102 ± 0.00226 (± 0.04%).
The age calculated from this $R^{FiC}/_{FC}$ value is: 315.36 ± 0.05 Ma (± 0.02%) 1σ analytical uncertainty, J-error included/ ± 0.55 Ma (± 0.17%) 1σ total uncertainty; n/tot = 4/8 (Fig. 6).

[a] $R^{FiC}/_{FC}$ values ± 1σ are calculated from weighted mean F values ± standard error of the weighted mean (Karner and Renne, 1998; Renne et al., 1998) of co-irradiated Fire Clay tonstein (FiC) and Fish Canyon (FC) sanidine. Ages and their associated uncertainties are calculated from R values relative to astronomically calibrated Fish Canyon monitor standard (Kuiper et al., 2008) as described in Section 2.2.
[b] Irradiation location identifier includes the irradiation number, disk letter and pit number (see Section 2.2); run ID is common to all analyses from the same irradiation pit (see Fig. A.1 for disk maps).
[c] ± 1σ is SEM, Standard Error of the weighted Mean.
[d] When any analysis was excluded n < tot (see Section 2.2 for exclusion procedures).
[e] Combined experiments from the same irradiation pit (Fig. 3C); total fusion analyses (n = 46) and B-steps (n = 30), total analyses = 76.
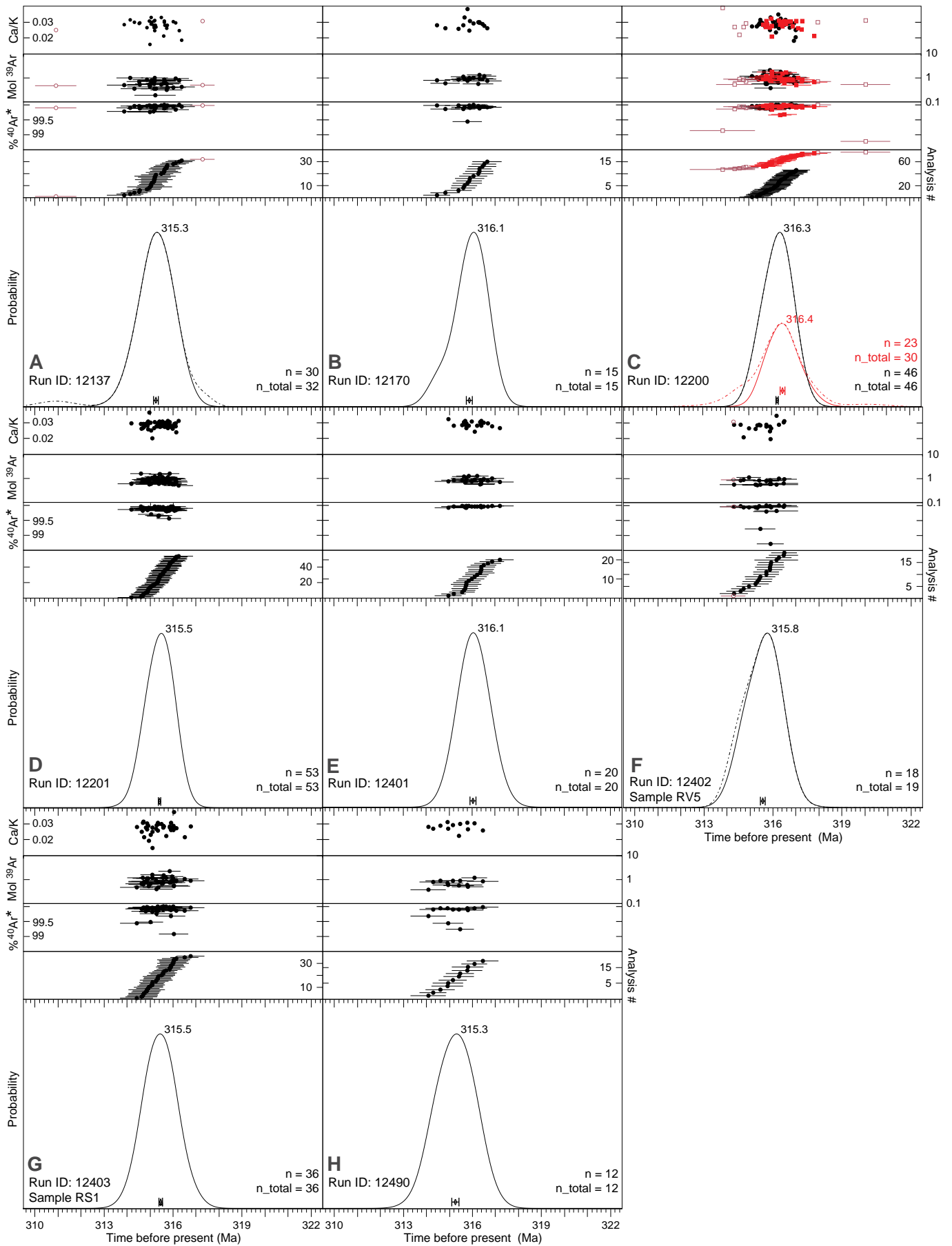
(caption on next page)

Fig. 3. $^{40}Ar/^{39}Ar$ single crystal sanidine date populations for Fire Clay tonstein and individual dates ± 1σ (analytical without J uncertainty, explained in Section 2.2), percent radiogenic Ar ($^{40}Ar*$), ^{39}Ar moles, and Ca/K ratios. All horizontal axes are identical and scaled to span about 4% of the mean date (same relative scales as in Fig. 4). A–H correspond to 8 irradiation pits with their unique Run ID numbers (Table 1). Open symbols indicate outliers excluded from the shown weighted mean, the dashed line represents the distribution if outliers were included and n_total is the total number of analyses before exclusions (see Section 2.2 for exclusion criteria). Mode date(s) are written above each curve, weighted mean dates (diamonds) ± 1σ are marked at the base.
Nine experiments are shown, representing different samples (sample RH1 unless otherwise noted) and variations in sanidine cleaning experiments (Appendix A and Table A.1). Two experiments are shown in C (Run ID 12200, Table 1): one includes total fusion analyses, the second includes high-power B-steps of a 2-step cleaning experiment (see Section 2.2 for symbols and details).

abrasion technique modified after Mattinson (2005) which involved annealing in a 900 °C furnace for 60 h, followed by acid leaching. For leaching, zircons were loaded with ~75 μl of 29 M HF in 200 μl FEP microcapsules, loaded in a Parr© vessel, and placed in a 210 °C oven for 12 h. In addition to effectively mitigating the effects of radiation-induced Pb loss in zircon, the chemical abrasion pre-treatment removes the persistent phyllosilicate coating of the grains, as well as any internal inclusions that might contain common lead. Following the leach, zircons were fluxed in a dilute HNO_3 solution and in 6 M HCl (1 h in each) in successive steps, with each step followed by 1 h of agitation in an ultrasonic cleaner, removal of the leachate and rinsing with MQ water. Thoroughly rinsed zircons were spiked with the EARTHTIME ET2535 mixed ^{202}Pb-^{205}Pb-^{233}U-^{235}U tracer (Condon et al., 2015; McLean et al., 2015), and totally dissolved in 29 M HF inside a Parr© vessel at 210 °C for 48 h. Following dissolution, the samples were dried to salts, and re-dissolved in ~50 μl of 6 M HCl at 180 °C for at least 12 h. Dissolved Pb and U were separated from the sample using an HCl-based anion exchange chemical procedure modified from Krogh (1973).

Both Pb and U were loaded together onto degassed zone-refined Re single filaments with a silica gel-H_3PO_4 emitter solution (Gerstenberger and Haase, 1997). The Pb and U isotopic ratios were measured on an Isotopx X62 multicollector thermal ionization mass spectrometer equipped with a Daly photomultiplier ion-counting system at MIT. Pb was measured by peak-hopping on a single Daly ion-counter whereas U was measured as an oxide in a static mode on 3 Faraday detectors. Data reduction, as well as calculation of dates and propagation of uncertainties were accomplished using the Tripoli and ETRedux software packages (Bowring et al., 2011; McLean et al., 2011). Age uncertainties are reported at 95% confidence level and, unless noted otherwise, in the ± *X/Y/Z* Ma format, where *X* is the analytical (internal) uncertainty only, *Y* includes *X* together with the tracer calibration uncertainties, and *Z* incorporates *Y* and the U decay constant uncertainties of Jaffey et al. (1971). For comparison between U-Pb and $^{40}Ar/^{39}Ar$ age data, *Z* must always be taken into account, whereas for comparison with U-Pb ID-TIMS results from other labs using the same tracer, only *X* is necessary.

3. Results

3.1. $^{40}Ar/^{39}Ar$

3.1.1. Internal precision and comparison with Fish Canyon standard

Single-crystal sanidine $^{40}Ar/^{39}Ar$ data from the Fire Clay tonstein (Fig. 3) show consistent precision across 9 different experiments varying in disaggregation methods, degree of residual kaolinite on crystals, cleaning methods, sample locations, and crystal shapes (Fig. 3, Appendix A and Table A.1). Only a few individual analyses were excluded from these experiments (11 out of total 263 analyses Table 1), mostly from a 2-step-heating experiment of crystals with slight kaolinite residue (Fig. 3C lower curve). The range for sanidine dates is ~315 Ma to ~317 Ma for these experiments, without the excluded individual analyses, or 314 to 317 Ma when all individual analyses are included (Fig. 3). These results have two implications for using the Fire Clay tonstein as a monitor standard: (1) DMSO solution does not affect the precision of individual dates, despite some persistent kaolinite residuals, because outliers can be easily identified and excluded, and (2)

DMSO disaggregation can generate large amounts of phenocrysts for interlaboratory distribution, because it provides an almost complete recovery of clean crystals.

Single-crystal sanidine $^{40}Ar/^{39}Ar$ data from co-irradiated Fish Canyon monitor standard (Fig. 4) show scatter similar to that of Fire Clay tonstein sanidines from the same irradiation pits (cf. Fig. 3) and slightly larger number of excluded analyses (15 out of 132 total analyses: Fig. 4). We further compared the scatter between date populations of Fish Canyon and Fire Clay (shown in Figs. 3 and 4) by looking at the ratio between the standard deviation of the mean for each population (no exclusions) divided by the respective mode (modes are shown on Figs. 3 and 4), plotted against the number of analyses per experiment (Fig. 5 and Table A.1). This estimate of scatter within most experiments of Fire Clay and Fish Canyon is < 0.23% of the mode regardless of the number of analyses, whereas two Fire Clay experiments have values between 0.3 and 0.4% of the mode and one Fish Canyon experiment has value of 0.56% of the mode.

The nine experiments presented here (Fig. 3) include two experiments on crystals from the same irradiation position (Run ID 12200: total fusion and B-step analyses, Fig. 3C). We combine the analyses of these two experiments into a single population and a single calculated weighted mean (Table 1, Run ID 12200) because the weighted mean dates of these two experiments overlap, despite the larger kaolinite coating of crystals subjected to 2-step heating. The eight experiments (Table 1) correspond to eight irradiation positions (Fig. A.1, A – H in Figs. 3 and 4). Full data for individual $^{40}Ar/^{39}Ar$ analyses are provided in Table A.2, following recommendations for data reporting of Renne et al. (2009).

3.1.2. Excluded experiments

Six experiments are excluded from age calculation for two different reasons. Two experiments of Fire Clay crystals treated with weak HF prior to analyses, still had residual kaolinite coating on some crystals. A subset of those crystals was subjected to additional cleaning by 2-step heating (rows 20–21 of Table A.1; Section 2.2). The results from these two experiments indicate that the combined cleaning treatments were too aggressive; Therefore, these experiments were excluded from the overall results (details in Appendix A).

The other four excluded experiments are monitors Taylor Creek sanidine and GA1550 biotite (rows 19, 22, 23 of Table A.1) and RH1 step heating experiment of 19 steps (Fig. A.5F). These experiments suffered analytical issues expressed as noticeable trends of ^{39}Ar moles with individual dates and show values of 0.6–0.7 for R^2 (Fig. A.9: A–B, G–H). Such trends suggest that the calculated mean from these date populations may be biased and therefore these experiments were excluded from the data used to calculate the best age estimate for the Fire Clay. We arbitrarily set the limit at R^2 larger than 0.5. Most experiments included in the age calculation (Table 1, Figs. 3–6), have R^2 values of zero (all Fire Clay data in Fig. A.7; four of eight Fish Canyon experiments in Fig. A.6A–D). The other four Fish Canyon experiments have R^2 values between 0.1 and 0.3 (Fig. A.6E–H). Respective R^2 values for correlating Ca/K ratios with individual dates are 0–0.3 for the four excluded experiments and are zero for all included experiments except a 0.1 value (Fish Canyon; Fig. A.6E). Details are provided in Appendix A.2, including correlation plots for all reported data (Figs. A.6–A.9).
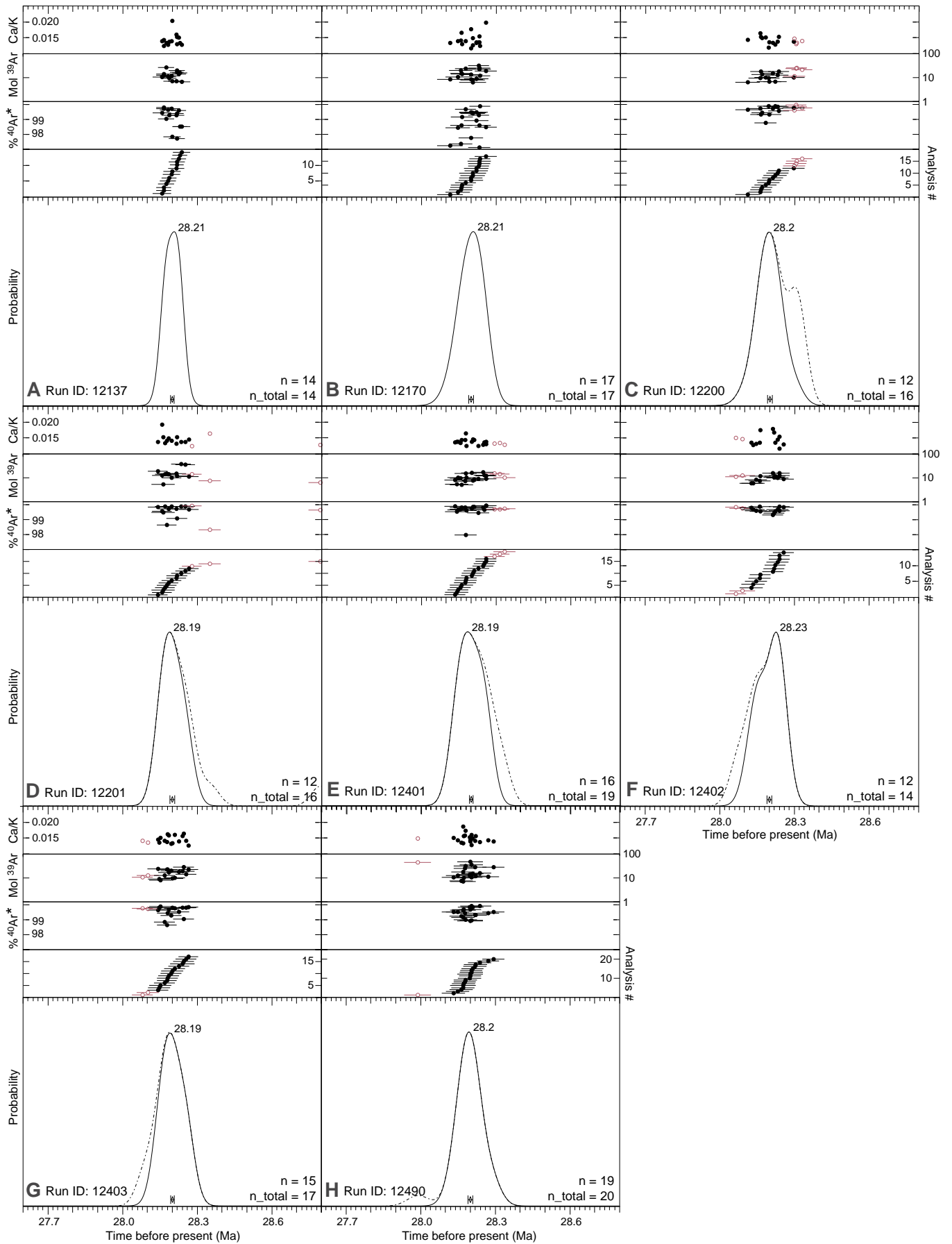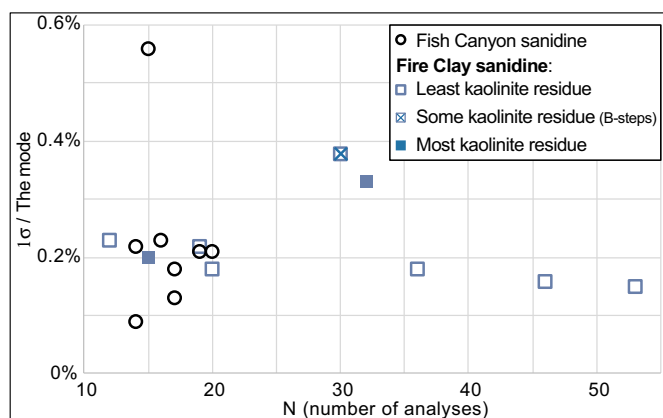
(caption on next page)

Fig. 4. Individual dates, derived from single sanidine analyses of co-irradiated Fish Canyon monitor in A–G. The individual dates within each irradiation pit (= each subplot) are calculated from the weighted mean J-value for the respective pit (Table 1) relative to Fish Canyon monitor age of 28.201 Ma (Kuiper et al., 2008), and thus are effectively the range of J-values from individual measurements. Subplots content, relative length of horizontal axes, uncertainty type and exclusion criteria are explained in Fig. 3 caption. One excluded individual run is not shown (subplot 4D: Ca/K > 0.025) but is listed in Table A.2.

3.1.3. *Weighted mean age of Fire Clay tonstein: accuracy*

Weighted mean dates from 8 Fire Clay ^{40}Ar/^{39}Ar experiments are spread beyond an obvious single population (MSWD = 9, probability = 0; Fig. 6). Geologic complexity is a possible explanation, but we think that laboratory procedures is a more likely reason. The youngest, clustered ages (Fig. 6) include the two furthermost locations of RH1 and RS1 (Fig. 1). The age of RV5 sample overlaps with RS1 although they are located > 100 km apart (Fig. 1). If any part of the K-Ar system was influenced depending on location, there is no evidence for it here although more ages of different locations would be required to thoroughly test if there is a link between age and location. We were attracted to the Fire Clay because Kunk and Rice (1994) reported remarkable consistent ages from step heating spectra of seven tonstein samples across > 300 km transect of mapped exposures (Fig. 1), although these samples were composed of ~100 mg sanidine separates in each sample. It is possible that some systematic variability in ages can be identified with more single-sanidine analyses (including step heating of single grains) from different sample locations.

Possible experimental causes for the observed spread are differences in sample preparation, analytical bias as described in Section 3.1.2 that may have affected certain experiments, and unaccounted for but systematic variations in neutron flux (J value). Sample preparation is unlikely the cause because there is no apparent relationship between the age values and dispersion with different preparation techniques. For example, the least-aggressive sample preparation with water includes both young and old weighted mean ages (12137, 12201, 12170; Fig. 6), and the most-aggressive preparation of initial disaggregation in warm DMSO for weeks followed by treatment with weak Hydrofluoric acid (12490, 12403, 12402, 12401; Fig. 6) also includes old and young ages. Cold room temperature (~15 °C–~18 °C) disaggregation on DMSO for several months yielded the single oldest measured age (12200; Fig. 6). Furthermore, one would expect sample preparation artifacts to affect sanidine crystals of different character variably, causing a noticeable spread of dates within such an experiment, but this is not seen in the data.

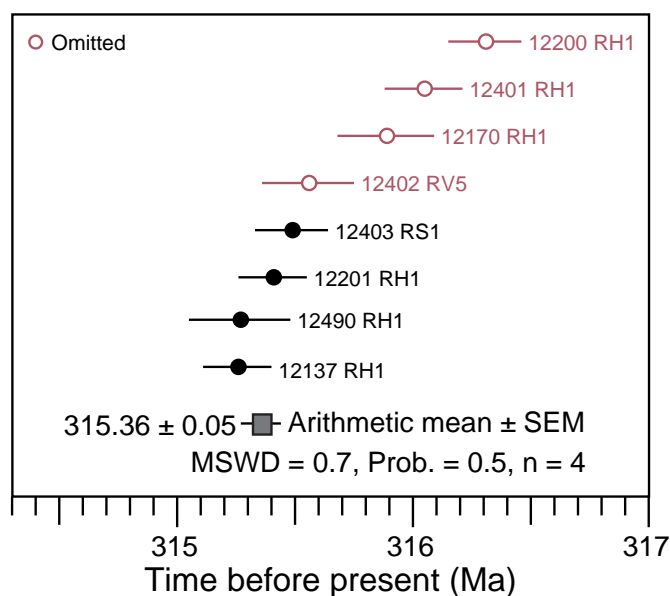Analytical bias such as correlated individual ages with signal strength for some experiments (Section 3.1.2) randomly appear at specific time periods within certain batch-analyses, and is not observed in the experiments reported in Table 1 and Fig. 6; therefore, we do not consider such analytical issues as a cause for the spread shown in Fig. 6. For example, within a 2+ weeks long batch-analysis some experiments suffered analytical bias and therefore were excluded and other experiments had no analytical issues (details in Appendix A.2).

We suspect that the observed scatter is Fig. 6 is due to a combination of vertical gradient of the neutron flux within irradiation pits and separation of Fire Clay grains at the bottom of the irradiation pit and Fish Canyon monitor sanidine at the top of the irradiation pits. In all irradiation pits grains were stacked in this order: Fire Clay sanidine at the bottom, followed by grains of 0–2 different standards and topped by Fish Canyon monitor standard sanidine. The J-value derived from Fish Canyon sanidines that are vertically separated from Fire Clay sanidine is biased in the presence of vertical neutron flux gradient, resulting in an apparent scatter of ages.

If our hypothesis is correct, we would expect that the least scattering of ages occurs when no or little vertical separation between Fire Clay and Fish Canyon grains exists and most scattering occurs for pits with the largest lengths of separations, as indeed we observe in Fig. 6. The 4 clustered youngest ages in Fig. 6 have the minimal amounts of separation between Fire Clay and Fish Canyon sanidine, whereas the 4 oldest and further scattered ages represent pits with the largest vertical separation. The 4 youngest ages are divided between irradiation pits 34C1 and 34C12 (12490, 12403 in Fig. 6; no separation between Fire Clay and Fish Canyon grains), and pits 29B9 and 32C10 (12137, 12201 in Fig. 6; ~24 grains of size 0.355–0.5 mm are loaded above Fire Clay grains creating a small separation). Larger amounts of separation occur in pits representing the older, more scattered ages. Those pits include: 34C6 and 34C4 (12402, 12401 in Fig. 6) where 30–40 GA1550 biotites are loaded above the Fire Clay grains, and pits 29A6 and 32C6 (12170, 12200 in Fig. 6) where 15–20 large grains are loaded above the Fire

Fig. 5. Comparison in data scatter between Fish Canyon and Fire Clay tonstein sanidine measurements. The scatter in dates expressed as 1σ/mode is calculated by taking the standard deviation of each date population without exclusions, and dividing it by the mode of the same population (modes ± 1σ are also listed in Table A.1). Included date populations are B-steps of a 2-step heating experiment (Fig. 3C) and 16 total fusion experiments in subplots A–H of both Figs. 3 and 4.

Fig. 6. Summary of weighted mean ^{40}Ar/^{39}Ar dates from 8 irradiations with 1σ analytical uncertainties including J-values errors (Table 1). Four weighted mean dates (solid circles) are used to calculate our preferred arithmetic mean age of 315.36 ± 0.05 (1σ, analytical including J uncertainty)/ ± 0.55 (1σ, total uncertainty) Ma for the Fire Clay tonstein sanidine (see Section 3.1.3, and Section 2.2 for uncertainty types).

Clay grains (1–2 mm grains from two internal lab standards; see Appendix A for details).

In light of this accuracy issue, only the irradiation pits with none/small grains separating the tonstein from Fish Canyon grains (and probably no/little in-pit vertical neutron flux gradient) are considered for the age calculation. Our preferred age of 315.36 ± 0.55 (± 0.17%, 1σ total uncertainty) Ma is the arithmetic mean ± standard error of the mean (SEM) for N = 4, from the 4 irradiation pits where in-pit vertical neutron flux gradients cannot compromise the results (Fig. 6). This age includes the youngest four weighted mean dates, with dates clustered together, and fits best with the hypothesis that in-pit neutron flux gradient caused the observed scatter depending on the vertical distance of stacked monitor crystals above Fire Clay crystals. The mean age from the two irradiation pits with no separation between Fire Clay and Fish Canyon sanidines in each pit is the same as our preferred age (315.39 ± 0.54 Ma; Run ID 12403 and 12490 in Fig. 6).

3.2. U-Pb

Forty-one single zircon grains were analyzed from sample RH1. Complete U-Pb data with their 2σ uncertainties are listed in Table A.4. The total amount of radiogenic Pb in the analyses ranged from 125 pg to 20 pg and that of U from 2.4 ng to 240 pg. $^{206}Pb/^{238}U$ dates (2σ internal error) of 28 elongate zircons with axial glass inclusions ranged from 314.25 ± 0.31 Ma to 314.80 ± 0.21 Ma (Figs. 2 and 7). Thirteen predominantly equant analyzed zircons ranged in $^{206}Pb/^{238}U$ dates from 314.98 ± 0.18 Ma to 961.55 ± 0.71 Ma indicating variable involvement of xenocrystic cores (Fig. A10). Average analytical precision was ± 0.23 Myr (0.14%). Our xenocrystic dates are consistent with previously published vintage U-Pb geochronology from the Fire Clay tonstein (Lyons et al., 2006; Rice et al., 1994) that showed strong discordance due to zircon inheritance.

The sample date representing the age of deposition of the tonstein is derived from the weighted mean $^{206}Pb/^{238}U$ date of a statistically coherent cluster of 28 youngest (elongate) zircon analyses that overlap within 2σ internal uncertainty (Fig. 7). The xenocrystic zircons producing resolvable older analyses can be objectively excluded from date calculation. The youngest cluster comprising 67% of our data yield a weighted mean $^{206}Pb/^{238}U$ date of 314.614 ± 0.038/0.090/0.35 Ma with a MSWD of 1.62. This MSWD reflects slightly higher data scatter outside of the 95% confidence interval (0.50 < MSWD < 1.54) due to one young analysis (z31) at 314.25 ± 0.19 Ma (Table A.4 and Fig. 7). Alternatively, excluding z31 would result in a weighted mean $^{206}Pb/^{238}U$ date of 314.629 ± 0.039/0.090/0.35 Ma with a MSWD of
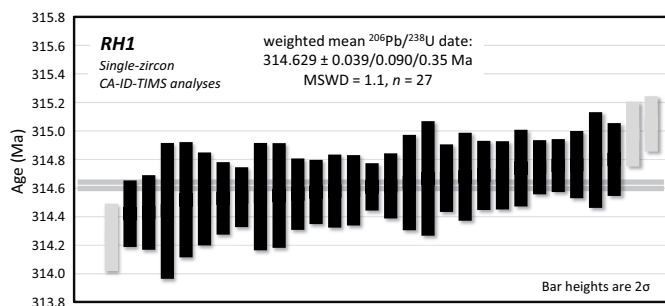
Fig. 7. Date distribution plot of the analyzed zircons from the Fire Clay tonstein sample RH1, showing 27 analyses included in age calculation (black bars) and excluded analyses (grey bars). Bar heights proportional to 2σ analytical uncertainty of individual analyses. Eleven other xenocrystic analyses plot outside the diagram and are not shown here. Background horizontal line and its grey envelope represent the calculated weighted mean date and its 95% confidence error envelope, respectively. Weighted mean uncertainty is expressed as ± X/Y/Z Ma as described in Section 2.3. See Table A.4 for complete U-Pb data and text for details of date uncertainties.

1.1. The two calculated dates overlap well within internal uncertainties and are thus statistically indistinguishable. We report the latter date as the interpreted age of the tonstein eruption.

Of the 13 significantly older, visibly outlying xenocrystic analyses that were excluded from age calculation, 9 regress to a discordia line (Fig. A.10) with a concordia upper intercept dates of 1017.6 ± 2.8 Ma (MSWD = 3.6). The upper intercept date points out to the Grenvillian age of the inherited zircon source (s), as indicated by previous U-Pb geochronology (Lyons et al., 2006; Rice et al., 1994).

4. Discussion

$^{40}Ar/^{39}Ar$ analyses of sanidine from the Fire Clay tonstein generated highly reproducible dates in each experiment within the analytical limits, across multiple sample locations (RH1, RS1, RV5) and degrees of cleaned crystals. Those results indicate that disaggregation in DMSO solution (as describe in Section 2.1) is sufficient to produce reproducible date populations and additional cleaning steps are not required (e.g., acid leaching and 2-step heating, Sections 2.1 and 2.2, respectively).

As discussed in Section 3.1.3, we use analyses from 4 irradiation pits with the least amount or no separation between tonstein and Fish Canyon grains to calculate an $^{40}Ar/^{39}Ar$ age of 315.36 ± 0.10 Ma (± 0.03%, 2σ analytical uncertainty) for the Fire Clay tonstein relative to an age of 28.201 Ma for Fish Canyon monitor (Kuiper et al., 2008). This age translates to an $^{40}Ar/^{39}Ar$ age 315.36 ± 1.10 Ma (2σ total uncertainty) that can be directly compared to U-Pb age for the same sample.

Our new U-Pb age of 314.629 ± 0.35 Ma (2σ total uncertainty) for the Fire Clay tonstein is based on a cluster of 27 single, chemically abraded, zircon analyses, for which all scatter in data can be reasonably explained by analytical dispersion. This date overlaps with a single, air-abraded, Fire Clay zircon date reported by Lyons et al. (2006), though our date is based on a much larger data set and with significantly improved analytical precision and EARTHTIME spike. Careful screening of Fire Clay zircon based on morphology and inclusions can effectively eliminate xenocrystic zircons and facilitate its use as a U-Pb reference material.

The new U-Pb age overlaps within total uncertainty with our preferred $^{40}Ar/^{39}Ar$ age reported here. However, this comparison is complicated by the limited precision of the $^{40}Ar/^{39}Ar$ mean age calculated here from several irradiations. Additionally, we acknowledge the yet to be completely resolved bias of ~1% between results from different $^{40}Ar/^{39}Ar$ labs (Heizler and the EARTHTIME working group, 2008). More analysis of the sanidines from multiple laboratories will be necessary to provide an accurate comparison between the two geochronometers, which would particularly benefit from experiments that also incorporate the measurement of the same gas standards with highly radiogenic argon isotopes and with ^{39}Ar. The results presented here indicate that the Fire Clay tonstein sanidine has good consistency of individual, single-crystal $^{40}Ar/^{39}Ar$ dates, and demonstrates the potential of the Fire Clay sanidine as a suitable Paleozoic monitor standard for $^{40}Ar/^{39}Ar$ geochronology.

Biostratigraphic constraints based on cephalopods and brachiopods from the marine strata below and above the Fire Clay bed allow correlation of this unit to the Westphalian B or Bolsovian substage (Middle Pennsylvanian Series) of western Europe (Rice et al., 1994). Davydov et al. (2010) presented high-precision U-Pb CA-ID-TIMS geochronology from the Carboniferous of the Donets Basin in eastern Ukraine that included a weighted mean $^{206}Pb/^{238}U$ date of 314.40 ± 0.06 Ma (2σ internal uncertainty) from a tonstein associated with the k3 coal unit. The k3 tonstein falls within the *Declinognathodus donetzianus* conodont zone that defines the base of the Moscovian Stage of the Pennsylvanian (Davydov et al., 2010). Our new U-Pb age of 314.629 ± 0.039 (internal uncertainty only) Ma thus provides direct temporal correlation between the Atokan stage of the North American mid-continent, the

Bolsovian substage of western Europe and the basal Muscovian Stage of the international time scale.

5. Summary and conclusions

Calibrating Earth history is an important task that underpins many disciplines within the Earth and planetary sciences. Obtaining accurate and precise radioisotopic ages requires not only rigorous attention to the analytical methodologies, but carefully designed experiments and well-characterized standards in order to explore systematic biases between geochronometers and laboratories. Sanidine from the Fire Clay tonstein shows remarkably consistent individual ^{40}Ar/^{39}Ar dates, giving a mean age of 315.36 ± 1.10 Ma (2σ total uncertainty), calculated from weighted mean ages of four irradiation positions. Although previous U-Pb geochronology from the Fire Clay tonstein was plagued by inherited zircons ranging up to ~1 Ga, careful morphological characterization of zircons allowed us to produce a geologically meaningful weighted mean ^{206}Pb/^{238}U date of 314.629 ± 0.35 Ma (2σ total uncertainty) based on 27 single, chemically abraded, zircon analyses. Although dates from the two chronometers are consistent within their fully propagated uncertainties, a detailed comparison between the two radioisotopic systems will be premature before further progress is made in overcoming the existing ^{40}Ar/^{39}Ar interlaboratory biases. Our results from the Fire Clay tonstein suggest that it is an ideal candidate for a mineral reference comparing ^{40}Ar/^{39}Ar and U-Pb geochronologies, in addition to serving as a robust correlation tie point for the Middle Pennsylvanian time scale.

Acknowledgments

Declaration of competing interest

The authors declare that they have no known competing financial interests or personal relationships that could have appeared to influence the work reported in this paper.

Appendix A. Supplementary data

Supplementary data include details of the following: Summary of all ^{40}Ar/^{39}Ar experiments, description of excluded experiments with evidence for analytical bias, description of sampling locations and distribution of mineral separates to other laboratories. Tables and figures of the supplementary data are: Tables A.1–4; Figs. A.1–A.13. Supplementary data to this article can be found online at https://doi.org/10.1016/j.chemgeo.2020.119485.

References

Black, L.P., Kamo, S.L., Allen, C.M., Davis, D.W., Aleinikoff, J.N., Valley, J.W., Mundil, R., Campbell, I.H., Korsch, R.J., Williams, I.S., Foudoulis, C., 2004. Improved 206Pb/238U microprobe geochronology by the monitoring of a trace-element-related matrix effect; SHRIMP, ID–TIMS, ELA–ICP–MS and oxygen isotope documentation for a series of zircon standards. Chem. Geol. 205, 115–140. https://doi.org/10.1016/j.chemgeo.2004.01.003.

Bowring, J.F., McLean, N.M., Bowring, S.A., 2011. Engineering cyber infrastructure for U-Pb geochronology: Tripoli and U-Pb_Redux. Geochemistry, Geophysics, Geosystems: G3 12. https://doi.org/10.1029/2010GC003479. Washington.

Cebula, G.T., Kunk, M.J., Mehnert, H.H., Naeser, C.W., Obradovich, J.D., Sutter, J.F., 1986. The Fish Canyon Tuff, a potential standard for the 40Ar-39Ar and fission-track dating methods. Terra Cognita 6, 139–140.

Chesnut, D.R., 1985. Source of volcanic ash deposit (flint clay) in the Fire Clay coal of the Appalachian basin. In: Tenth International Congress for Carboniferous Stratigraphy and Geology, pp. 145–154 Compte Rendu 1.

Condon, D.J., McLean, N., Noble, S.R., Bowring, S.A., 2010. Isotopic composition (238U/235U) of some commonly used uranium reference materials. Geochim. Cosmochim. Acta 74, 7127–7143. https://doi.org/10.1016/j.gca.2010.09.019.

Condon, D.J., Schoene, B., McLean, N.M., Bowring, S.A., Parrish, R.R., 2015. Metrology and traceability of U–Pb isotope dilution geochronology (EARTHTIME Tracer Calibration Part I). Geochim. Cosmochim. Acta 164, 464–480. https://doi.org/10.1016/j.gca.2015.05.026.

Davydov, V.I., Crowley, J.L., Schmitz, M.D., Poletaev, V.I., 2010. High-precision U-Pb zircon age calibration of the global Carboniferous time scale and Milankovitch band cyclicity in the Donets Basin, eastern Ukraine. Geochem. Geophys. Geosyst. 11. https://doi.org/10.1029/2009GC002736.

Ganerød, M., Chew, D.M., Smethurst, M.A., Troll, V.R., Corfu, F., Meade, F., Prestvik, T., 2011. Geochronology of the Tardree Rhyolite Complex, Northern Ireland: implications for zircon fission track studies, the North Atlantic Igneous Province and the age of the Fish Canyon sanidine standard. Chem. Geol. 286, 222–228. https://doi.org/10.1016/j.chemgeo.2011.05.007.

Gerstenberger, H., Haase, G., 1997. A highly effective emitter substance for mass spectrometric Pb isotope ratio determinations. Chem. Geol. 136, 309–312. https://doi.org/10.1016/S0009-2541(96)00033-2.

Heizler, M., the EARTHTIME working group, 2005. Evaluating intercomparability amongst several 40Ar/39Ar laboratories. Geochim. Cosmochim. Acta 69, A318.

Heizler, M., the EARTHTIME working group, 2008. Argon laboratory intercomparison efforts for the Earthtime initiative. Geophys. Res. Abstr. 10, EGU2008-A-11478.

Hess, J.C., Lippolt, H.J., Burger, K., 1988. New time-scale calibration points in the upper Carboniferous from Kentucky, Donetz basin, Poland, and West Germany. 6th Workshop on Fission Track Dating September 5 – 9, 1988: Besançon, France.

Hiess, J., Condon, D.J., McLean, N., Noble, S.R., 2012. 238U/235U Systematics in terrestrial uranium-bearing minerals. Science 335, 1610–1614. https://doi.org/10.1126/science.1215507.

Huddle, J.W., Englund, K.J., 1966. Geology and Coal Reserves of the Kermit and Varney Area, Kentucky (USGS Numbered Series No. 507). Professional Paper. U.S. Govt. Print. Off. https://doi.org/10.3133/pp507.

Jaffey, A.H., Flynn, K.F., Glendenin, L.E., Bentley, W.C., Essling, A.M., 1971. Precision measurement of half-lives and specific activities of 235U and 238U. Phys. Rev. C 4, 1889–1906. https://doi.org/10.1103/PhysRevC.4.1889.

Karner, D.B., Renne, P.R., 1998. 40Ar/39Ar geochronology of Roman volcanic province tephra in the Tiber River valley: age calibration of middle Pleistocene sea-level changes. GSA Bull. 110, 740–747. https://doi.org/10.1130/0016-7606(1998)110<0740:AAGORV>2.3.CO;2.

Krogh, T.E., 1973. A low-contamination method for hydrothermal decomposition of zircon and extraction of U and Pb for isotopic age determinations. Geochim. Cosmochim. Acta 37, 485–494. https://doi.org/10.1016/0016-7037(73)90213-5.

Kuiper, K.F., Deino, A., Hilgen, F.J., Krijgsman, W., Renne, P.R., Wijbrans, J.R., 2008. Synchronizing rock clocks of Earth history. Science 320, 500–504. https://doi.org/10.1126/science.1154339.

Kunk, M.J., Rice, C.L., 1994. High-precision 40Ar/39Ar age spectrum dating of sanidine from the Middle Pennsylvanian Fire Clay tonstein of the Appalachian basin. In: Rice, C.L. (Ed.), Elements of Pennsylvanian Stratigraphy, Central Appalachian Basin. Geological Society of America Special Paperspp. 105–114. https://doi.org/10.1130/SPE294-p105.

Lee, J.-Y., Marti, K., Severinghaus, J.P., Kawamura, K., Yoo, H.-S., Lee, J.B., Kim, J.S., 2006. A redetermination of the isotopic abundances of atmospheric Ar. Geochim. Cosmochim. Acta 70, 4507–4512. https://doi.org/10.1016/j.gca.2006.06.1563.

Lipman, P.W., Bachmann, O., 2015. Ignimbrites to batholiths: integrating perspectives from geological, geophysical, and geochronological data. Geosphere 11, 705–743. https://doi.org/10.1130/GES01091.1.

Lyons, P.C., Outerbridge, W.F., Triplehorn, D.M., Evans Jr., H.T., Congdon, R.D., Capiro, M., Hess, J.C., Nash, W.P., 1992. An Appalachian isochron: a kaolinized Carboniferous air-fall volcanic-ash deposit (tonstein). GSA Bull. 104, 1515–1527. https://doi.org/10.1130/0016-7606(1992)104<1515:AAIAKC>2.3.CO;2.

Lyons, P.C., Krogh, T.E., Kwok, Y.Y., Davis, D.W., Outerbridge, W.F., Evans, H.T., 2006. Radiometric ages of the Fire Clay tonstein [Pennsylvanian (Upper Carboniferous), Westphalian, Duckmantian]: a comparison of U–Pb zircon single-crystal ages and 40Ar/39Ar sanidine single-crystal plateau ages. Int. J. Coal Geol. 67, 259–266. https://doi.org/10.1016/j.coal.2005.12.002.

Mattinson, J.M., 2005. Zircon U–Pb chemical abrasion ("CA-TIMS") method: combined annealing and multi-step partial dissolution analysis for improved precision and accuracy of zircon ages. Chem. Geol. 220, 47–66. https://doi.org/10.1016/j.chemgeo.2005.03.011.

Mattinson, J.M., 2010. Analysis of the relative decay constants of 235U and 238U by multi-step CA-TIMS measurements of closed-system natural zircon samples. Chem. Geol. 275, 186–198. https://doi.org/10.1016/j.chemgeo.2010.05.007.

McLean, N.M., Bowring, J.F., Bowring, S.A., 2011. An algorithm for U-Pb isotope dilution data reduction and uncertainty propagation. Geochemistry, Geophysics, Geosystems: G3 12 https://doi.org/10.1029/2010GC003478. Washington.

McLean, N.M., Condon, D.J., Schoene, B., Bowring, S.A., 2015. Evaluating uncertainties in the calibration of isotopic reference materials and multi-element isotopic tracers (EARTHTIME Tracer Calibration Part II). Geochim. Cosmochim. Acta 164, 481–501. https://doi.org/10.1016/j.gca.2015.02.040.

Mercer, C.M., Hodges, K.V., 2016. ArAR—a software tool to promote the robust comparison of K–Ar and 40Ar/39Ar dates published using different decay, isotopic, and monitor-age parameters. Chem. Geol. 440, 148–163. https://doi.org/10.1016/j.chemgeo.2016.06.020.

Min, K., Mundil, R., Renne, P.R., Ludwig, K.R., 2000. A test for systematic errors in 40Ar/39Ar geochronology through comparison with U/Pb analysis of a 1.1-Ga rhyolite. Geochim. Cosmochim. Acta 64, 73–98. https://doi.org/10.1016/S0016-7037(99)00204-5.

Ogg, J.G., Ogg, G.M., Gradstein, F.M., 2016. 1- Introduction. In: Ogg, J.G., Ogg, G.M., Gradstein, F.M. (Eds.), A Concise Geologic Time Scale. Elsevier, pp. 1–8. https://doi.org/10.1016/B978-0-444-59467-9.00001-7.

Ramezani, J., Hoke, G.D., Fastovsky, D.E., Bowring, S.A., Therrien, F., Dworkin, S.I., Atchley, S.C., Nordt, L.C., 2011. High-precision U-Pb zircon geochronology of the Late Triassic Chinle Formation, Petrified Forest National Park (Arizona, USA): Temporal constraints on the early evolution of dinosaurs. GSA Bull. 123, 2142–2159. https://doi.org/10.1130/B30433.1.

Renne, P.R., Swisher, C.C., Deino, A.L., Karner, D.B., Owens, T.L., DePaolo, D.J., 1998. Intercalibration of standards, absolute ages and uncertainties in 40Ar/39Ar dating. Chem. Geol. 145, 117–152. https://doi.org/10.1016/S0009-2541(97)00159-9.

Renne, P.R., Deino, A.L., Hames, W.E., Heizler, M.T., Hemming, S.R., Hodges, K.V., Koppers, A.A.P., Mark, D.F., Morgan, L.E., Phillips, D., Singer, B.S., Turrin, B.D., Villa, I.M., Villeneuve, M., Wijbrans, J.R., 2009. Data reporting norms for 40Ar/39Ar geochronology. Quaternary Geochronology, Dating the Recent Past 4, 346–352. https://doi.org/10.1016/j.quageo.2009.06.005.

Renne, P.R., Mundil, R., Balco, G., Min, K., Ludwig, K.R., 2010. Joint determination of 40K decay constants and 40Ar*/40K for the Fish Canyon sanidine standard, and improved accuracy for 40Ar/39Ar geochronology. Geochim. Cosmochim. Acta 74, 5349–5367. https://doi.org/10.1016/j.gca.2010.06.017.

Renne, P.R., Balco, G., Ludwig, K.R., Mundil, R., Min, K., 2011. Response to the comment by W.H. Schwarz et al. on "Joint determination of 40K decay constants and 40Ar*/40K for the Fish Canyon sanidine standard, and improved accuracy for 40Ar/39Ar

geochronology" by P.R. Renne et al. (2010). Geochim. Cosmochim. Acta 75, 5097–5100. https://doi.org/10.1016/j.gca.2011.06.021.

Rice, C.L., Belkin, H.E., Henry, T.W., Zartman, R.E., Kunk, M.J., 1994. The Pennsylvanian Fire Clay tonstein of the Appalachian basin—its distribution, biostratigraphy, and mineralogy. Geol. Soc. Am. Spec. Pap. 294, 87–104. https://doi.org/10.1130/SPE294-p87.

Schmitz, M.D., 2012. Appendix 2- radiometric ages used in GTS2012. In: Gradstein, F.M., Ogg, J.G., Schmitz, Mark D., Ogg, G.M. (Eds.), The Geologic Time Scale. Elsevier, Boston, pp. 1045–1082. https://doi.org/10.1016/B978-0-444-59425-9.15002-4.

Sinha, A.K., Zietz, I., 1982. Geophysical and geochemical evidence for a Hercynian magmatic arc, Maryland to Georgia. Geology 10, 593–596. https://doi.org/10.1130/0091-7613(1982)10<593:GAGEFA>2.0.CO;2.

Sláma, J., Košler, J., Condon, D.J., Crowley, J.L., Gerdes, A., Hanchar, J.M., Horstwood, M.S.A., Morris, G.A., Nasdala, L., Norberg, N., Schaltegger, U., Schoene, B., Tubrett, M.N., Whitehouse, M.J., 2008. Plešovice zircon — a new natural reference material for U–Pb and Hf isotopic microanalysis. Chem. Geol. 249, 1–35. https://doi.org/10.1016/j.chemgeo.2007.11.005.

Steiger, R.H., Jäger, E., 1977. Subcommission on geochronology: convention on the use of decay constants in geo- and cosmochronology. Earth Planet. Sci. Lett. 36, 359–362. https://doi.org/10.1016/0012-821X(77)90060-7.

Stevens, S., 1979. Petrogenesis of a Tonstein in the Appalachian Bituminous Basin (M.S. Thesis). Eastern Kentucky University.

Triplehorn, D.M., 2002. An easy way to remove fossils from sandstones: DMSO disaggregation. J. Paleontol. 76, 394–395. https://doi.org/10.1666/0022-3360(2002)076<0394:AEWTRF>2.0.CO;2.

Triplehorn, D.M., Bohor, B.F., Betterton, W.J., 2002. Chemical disaggregation of kaolinitic claystones (tonsteins and flint clays). Clay Clay Miner. 50, 766–770. https://doi.org/10.1346/000986002762090164.

Wanless, H.R., 1946. Pennsylvanian geology of a part of the southern Appalachian coal field. In: Geological Society of America Memoirs. Geological Society of America. https://doi.org/10.1130/MEM13.